

A relativistic approach to the "Dark Matter" effect, and some of its features and consequences.

José B. Almeida

*Universidade do Minho, Departamento de Física, 4710-057 Braga, Portugal.**

Roger Y. Gouin

Independent Scholar, 9230 Burt St. No. 309, Omaha NE 68114, USA.†

(Dated: September 12, 2003)

Insert abstract.

I. INTRODUCTION

It is generally argued that the rotation velocity curve of spiral galaxies must be explained through recourse to undetectable "dark matter" (Silk, 1997), the argument being that the observed orbital velocity is constant at large distances from the center (e.g. Rubin *et al.*, 1978) so, since the gravitational pull must balance the centrifugal force, one should have for any orbiting star

$$\frac{GmM}{r^2} = \frac{mv^2}{r}, \quad (1)$$

where G is the gravitational constant, m is the star's mass, M the total mass inside the orbit, r the orbital radius and v the star's linear velocity. If the observed velocity is roughly independent from r , one concludes that the mass must grow proportionally to r , which is in marked contrast with the observed mass distribution and leads to the conclusion that there must be a massive amount of matter present but undetectable with our present instruments. Of course such an approach requires arbitrarily adjusting the unseen matter features to fit observed data.

In order to avoid this state of affairs, a modification of Newton dynamics (given the acronym MOND) has been proposed by Milgrom (Milgrom, 1983a,b) and has been tested against the measured rotation velocities of several galaxies, proving able to explain the velocity curves with mass distributions following closely the actually observed distributions (Sanders, 1996). Successful as it is, MOND suffers from two main shortcomings: (a) it still has empirical features, one adjustable parameter and one adjustable function and (b) it is non-relativistic.

In the following presentation the authors propose an alternative to Newton's gravitational law for galaxy-scale mass distributions which (a) can be derived from a relativistic space metric, (b) disagrees with the MOND approach as it predicts an edge to the mass distribution beyond which Newton's Law applies (no need to go against GR), and (c) is consistent with the Dark Matter approach by obtaining a similar total mass of

the distribution. This approach does not suffer from parameter and function adjustments in order to fit the observations.

In marked contrast with the other approaches, this theory is found falsifiable as it predicts (a) an observable edge to the mass distributions beyond which Newton's Law must apply, (b) optical illusions affecting certain observations of galaxies (unreachable via Newton's Law), (c) certain observable active galactic nuclei effects, and (d) the kind of luminosity profile that necessarily results from a known H_I profile. All such predictions are unreachabe through the other existing approaches.

II. A NEW GRAVITATIONAL LAW

Eq. (1), known as the virial equation, is based on Newton's Mechanics which states that the gravitational potential of a mass M is

$$V = \frac{GM}{r}. \quad (2)$$

This allows the virial equation to be written in the alternative form

$$\frac{v^2}{r} = -\frac{dV}{dr}; \quad (3)$$

where V is taken as a central potential, i.e. only dependent on r . In terms of the angular velocity $\omega = v/r$,

$$\omega^2 = -\frac{1}{r} \frac{dV}{dr}. \quad (4)$$

When considering a radial mass distribution that encompasses the orbiting body instead of a central mass, it is not indifferent to use Eqs. (1) or (3) because

$$\frac{M(r)}{r^2} \neq -\frac{d}{dr} \left[\frac{M(r)}{r} \right]. \quad (5)$$

In fact, application of Newton's law would imply $v^2/r = \phi$, where ϕ verifies the Poisson equation

$$\nabla^2 \phi = \rho, \quad (6)$$

with ρ the density of the mass distribution.

*Electronic address: bda@fisica.uminho.pt

†Electronic address: rgouin@mindspring.com

The authors are proposing a replacement for Eq. (4), compatible with Newton's law of gravitation in a general situation but derived from space-time curvature and able to explain large-scale mass distributions dynamics inferred from galaxy disk luminosity observations without recourse to hidden mass (dark matter). The proposed equation is

$$\omega^2 = \frac{-1}{re^{2V/c^2}} \frac{dV}{dr}. \quad (7)$$

This equation can be tested for orbits around a central body where the gravitational potential should still be given by Eq. (2). If this potential is inserted into Eq. (7) one gets

$$\omega^2 = \frac{GM}{r^3 e^{2GM/c^2 r}}. \quad (8)$$

Notice the appearance of the factor $\exp(2GM/c^2 r)$ in the denominator. In normal circumstances Eq. (8) will evaluate to nearly the same angular velocity as results from Newton's law. The exponential of the denominator in the second member can be assumed to be unity in orbits around central bodies when the distance to the center is always large compared to GM/c^2 , but the same should not happen for the vicinity of a black hole (Martin, 1988) or for the nucleus of galaxies.

If Eq. (7) is now used with a radially continuous mass one gets

$$\omega^2 = \frac{G}{r^3 e^{2GM/c^2 r}} \left(M - r \frac{dM}{dr} \right); \quad (9)$$

resulting in an equation for the rotation velocity that departs radically from the virial equation (1)

$$v^2 = \frac{G}{r e^{2GM/c^2 r}} \left(M - r \frac{dM}{dr} \right). \quad (10)$$

In principle it will be possible to replace the first member of this equation with the square of an observed velocity law and obtain the mass distribution by integration. In real situations this will imply numerical integration due to the impossibility of describing analytically most observed rotation velocity laws.

A quick look at the equation above will show that in most circumstances the exponential can be made equal to unity and the parenthesis is actually the dominant factor. In the majority of circumstances the continuous aspect of the distribution is the key, and it will be indifferent to use Eq. (10) or Eq. (3) with the potential given by Eq. (2); the main advantage of the former is the fact that it can be derived from GR space metric, as will be shown below. The authors show also the perfect consistency between the metric leading to Eq. (10) and the molecular induced space curvature that explains the observed warping of galaxies' disks.

Trying to get some general indications about the shape of mass distributions that can produce observed velocity curves, we isolate the derivative

$$\frac{dM}{dr} \approx \frac{M}{r^2} - \frac{v^2}{G}. \quad (11)$$

Mass must be a monotonic function of distance in order to avoid meaningless negative densities; this means that the first term on the second member must always prevail over the second term. Since velocities tend to reach a stationary value and mass should not grow indefinitely, it is expected that the two terms balance each other at some distance where a smooth transition to space outside the continuous mass distribution can be made.

III. THE RELATIVISTIC BASIS OF THE NEW LAW

We are showing here that the proposed angular velocity Eq. (7) can be deduced from the relativistic space metric postulated below ¹

$$ds^2 = c^2 e^{-2V/c^2} dt^2 - (dx^2 + dy^2 + dz^2), \quad (12)$$

where V is the Newtonian central potential given by Eq. (2) and M can be a function of r . Only stationary sources are considered here (following Schwarzschild's assumption) (Schwarzschild, 1916).

The Lagrangian can be defined by

$$2L = c^2 e^{-2V/c^2} \left(\frac{dt}{ds} \right)^2 - \left(\frac{dx}{ds} \right)^2 - \left(\frac{dy}{ds} \right)^2 - \left(\frac{dz}{ds} \right)^2; \quad (13)$$

with the Lagrangian constant and equal to 1/2. The problem has cylindrical symmetry so it is useful to change into spherical coordinates

$$2L = c^2 e^{-2V/c^2} \left(\frac{dt}{ds} \right)^2 - \left(\frac{dr}{ds} \right)^2 - r^2 \left[\left(\frac{d\theta}{ds} \right)^2 + \sin^2 \theta \left(\frac{d\varphi}{ds} \right)^2 \right]. \quad (14)$$

From the Lagrangian one derives immediately the conjugate momenta associated with each of the generalized coordinates:

$$\begin{aligned} p_t &= c^2 e^{-2V/c^2} \frac{dt}{ds} \\ p_r &= -\frac{dr}{ds}, \\ p_\theta &= -r^2 \frac{d\theta}{ds}, \\ p_\varphi &= -r^2 \sin^2 \theta \frac{d\varphi}{ds}. \end{aligned} \quad (15)$$

For radial trajectories both θ and φ are constants and consequently $p_\theta = p_\varphi = 0$.

¹ Although the metric is postulated here without justification, this can be found in (Almeida, 2001)

The canonical equations are generally written as

$$\frac{dp_i}{ds} = \frac{\partial L}{\partial x_i}, \quad (16)$$

with p_i standing for $p_t, p_r, p_\theta, p_\varphi$ and x_i standing for t, r, θ, φ , respectively. The radial equation is

$$\begin{aligned} \frac{d^2 r}{ds^2} = & -e^{-2V/c^2} \frac{dV}{dr} \left(\frac{dt}{ds} \right)^2 \\ & - r \left(\frac{d\theta}{ds} \right)^2 - r \sin^2 \theta \left(\frac{d\varphi}{ds} \right)^2; \end{aligned} \quad (17)$$

noting that

$$\frac{d^2 r}{ds^2} = \frac{d^2 r}{dt^2} \left(\frac{dt}{ds} \right)^2, \quad (18)$$

dividing both members in Eq. (17) by $(dt/ds)^2$ and rearranging, with θ and φ constant,

$$e^{2V/c^2} \frac{d^2 r}{dt^2} = -\frac{dV}{dr}. \quad (19)$$

In the limit, if M is a central mass, thus independent from r , Eq. (19) reduces to

$$e^{2GM/c^2 r} \frac{d^2 r}{dt^2} = \frac{GM}{r^2}. \quad (20)$$

The exponential factor in the first member is usually very nearly unity, notice that $c^2/2GM$ is the radius of a black hole horizon, so that Eq. (20) is effectively equivalent to Newton's dynamics in the majority of situations. In continuous mass distributions, though, one is dealing with values of r that tend to zero and the exponential factor acquires a crucial importance.

With circular orbits, one can make $\theta = \pi/2$ in the radial equation (17) and simultaneously make the replacement

$$\frac{d\varphi}{ds} = \frac{d\varphi}{dt} \frac{dt}{ds} = \omega \frac{dt}{ds}, \quad (21)$$

to get

$$\frac{d^2 r}{ds^2} = - \left(e^{-2V/c^2} \frac{dV}{dr} + r\omega^2 \right) \left(\frac{dt}{ds} \right)^2. \quad (22)$$

In a circular orbit the first member of the equation is zero and one gets Eqs. (7) and (9), thereby confirming the relativistic form of the proposed new gravitation law for angular velocity. This law was also shown earlier to match Newton's in circumstances not involving mass distributions.

IV. ON THE MOND APPROACH

The question now arises on how MOND fares in comparison to the present proposal. According to Milgrom (Milgrom, 1983b), one should use an acceleration given by

$$g\mu(g/a_0) = g_N, \quad (23)$$

where g_N is the acceleration according to Newton, a_0 is an acceleration parameter, g is the actual acceleration and $\mu(x)$ is a function whose value is x for $x \ll 1$ and becomes unity for $x \gg 1$. Basically one has two limiting situations: for large g this function is GM/r^2 , as usual, but for small g one has

$$g = \frac{\sqrt{a_0 GM}}{r}. \quad (24)$$

When this acceleration is used in conjunction with the virial equation, one gets immediately $v_m^2 = \sqrt{a_0 GM_t}$ for large distances with M_t being the total mass of the galaxy.

For comparison with Eq. (10) one has to make $dM/dr = 0$, because at the edge of the galaxy the mass should not grow any further. One also replaces the exponential by unity, which is certainly legitimate at these distances, and then, equating MOND's estimation to the authors' (and Newton's), with r_0 the edge radius $\sqrt{a_0 GM_t} = GM_t/r_0$ and finally $a_0 = GM_t/r_0^2$. If, as Milgrom suggests, a_0 is a constant, this implies that all galaxies have similar average surface densities, a conclusion which is not supported by observations, witness Low Surface Brightness (LSB) galaxies where MOND gets too low surface densities unless a_0 is adjusted. We shall see below that the proposed space metric and the resulting gravitational law do not require any adjustment to match observations.

Incidentally, notice that the total mass estimated by the author's model coincides with the mass estimated by conventional means to be internal to the last measured point, if this happens to be very near the edge. In fact, when one zeroes the derivative in Eq. (10) and considers the exponential to be unity, this equation becomes equivalent to the virial equation. Since the edge is the distance where mass gets to its maximum value and measurements are made as close as possible to this distance, the velocities estimated by the two methods must be similar, although the corresponding mass distributions are very different.

V. TESTING THE MODEL

One can make predictions with the model by inserting any radially dependent orbital velocity in the first member of Eq. (10) and integrating the resulting differential equation.

A. Theoretical Cases

Three different idealized situations are analyzed next in order to allow a proper understanding of real galaxy studies.

Stationary rotational velocity

The most critical situation arises when one tries to obtain a constant velocity as observed near the edge in many galaxies. As an example we insert the following velocity law into Eq.

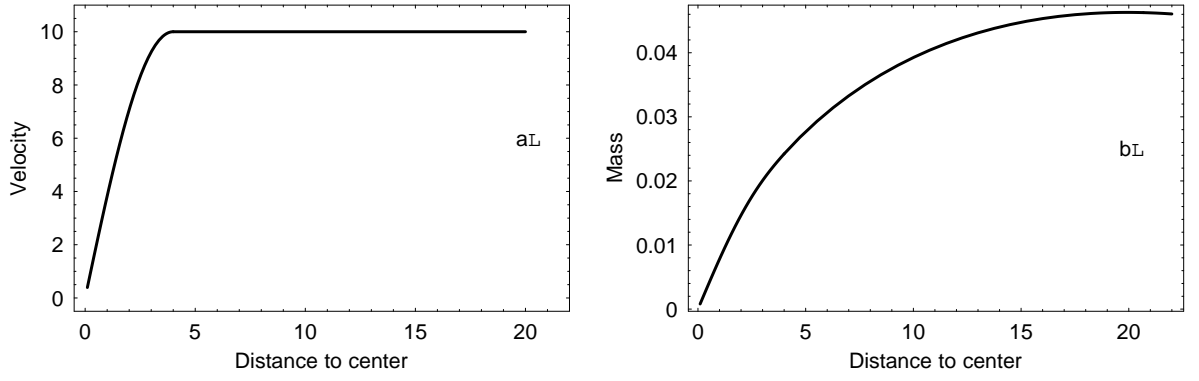


FIG. 1 Theoretical model with an extended flat rotation curve; velocity in Km/s, mass $10^{10} M_{\odot}$ and distance in kpc.

(10)

$$\begin{aligned} v &= 10 \sin\left(\frac{\pi}{8}r\right), \quad r < 4; \\ v &= 10, \quad r \geq 4; \end{aligned} \quad (25)$$

velocity is in Km/s and distance in kpc

The integration process introduces one constant which is set as the mass internal to a given radius; in the present example, the mass internal to 10 pc was set to $7.97 \times 10^5 M_{\odot}$. After integration, the mass at any distance is given by two different analytical expressions:

$$\begin{aligned} M &= -1.04 \times 10^6 r \ln[1 - 1.11 \times 10^{-9} \\ &\quad \times (\text{Ci } 0.79r - \ln r)], \quad r < 4; \\ M &= -1.04 \times 10^6 r \\ &\quad \times \ln(1 + 2.22 \times 10^{-9} \ln r), \quad r \geq 4; \end{aligned} \quad (26)$$

”Ci” represents the cosine integral function (Abramowitz and Stegun, 1970), mass is in $10^{10} M_{\odot}$ and distance in kpc.

If Eq. (3) had been used in place of Eq. (10) the mass distribution would differ from the above in less than one part in 10^9 :

$$\begin{aligned} M &= 0.00116r (6.52 + \text{Ci } 0.79r - \ln r), \quad r < 4; \\ M &= 0.00232r (3.99 - \ln r), \quad r \geq 4. \end{aligned} \quad (27)$$

The rotation velocity and mass distribution are plotted in Fig. 1. At a distance around 20 kpc the mass reaches a maximum of $4.7 \times 10^8 M_{\odot}$ and starts declining; since a decreasing mass would imply a negative density, the distance where mass reaches its maximum is chosen as the galaxy’s edge; a different choice for the mass internal to 10 kpc would have led to a peak of the mass distribution at a different distance, as discussed in another example. From the edge onwards mass should remain constant but it is no longer reasonable to speak of rotation velocity because there is nothing to rotate; consequently the rotation velocity curve must be stopped at the point where the mass peaks. Contrary to Newtonian based derivations, one concludes that mass does not grow to infinity in order to sustain a constant rotational velocity.

A reversed example

The next example imposes a mass distribution which reasonably mimics the mass curves found for some galaxies via the expression

$$\begin{aligned} M &= 10^{-4} (e^{-r/12.5} - e^{-r/10}), \quad r < 11.2; \\ M &= 8.19 \times 10^{-6}, \quad 11.2 \leq r < 12.5; \\ M &= 8.4 \times 10^{-6}, \quad r \geq 12.5; \end{aligned} \quad (28)$$

where mass is in $10^{10} M_{\odot}$ and distance in kpc. This mass profile is shown in Fig. 2 b) and is similar to what was found for DDO 154, later in this text. Eqs. (28) represent a continuous mass distribution, resulting possibly from a gas cloud and baryonic matter. The continuous cloud extends to 11.16 kpc beyond which distance mass remains essentially constant, except for an isolated star which was included at 12.5 kpc.

If a disk shape is assumed for the galaxy, the mass M internal to a distance r can be related to the surface density σ by the formula

$$M = \int_0^r 2\pi r' \sigma dr', \quad (29)$$

where the surface density is taken as dependent on r' only. The surface density was found by derivation of the mass curve, followed by division by $2\pi r$, and is represented in Fig. 2 c). The main point to notice is the singularity in the center, resulting from the division by r ; only a mass curve with zero slope at the center portion could avoid the singularity but this would lead to difficulties in the velocity determination in this area.

Rotation velocity was determined by application of Eq. (10) and is plotted in Fig. 2 a). The velocity rises steeply from the center stabilizes near the end of the continuous cloud. The curve is continuous on the edge of the gas cloud but changes slope abruptly into approximately a Keplerian $r^{-1/2}$ decline. This is a region where there is no mass and so the rotation curve is merely theoretical, however, an external star, with a small mass compared to the galaxy’s total mass, will rotate according to this curve. As explained later, it is expected that external stars of NGC 247 lie on a similar curve.

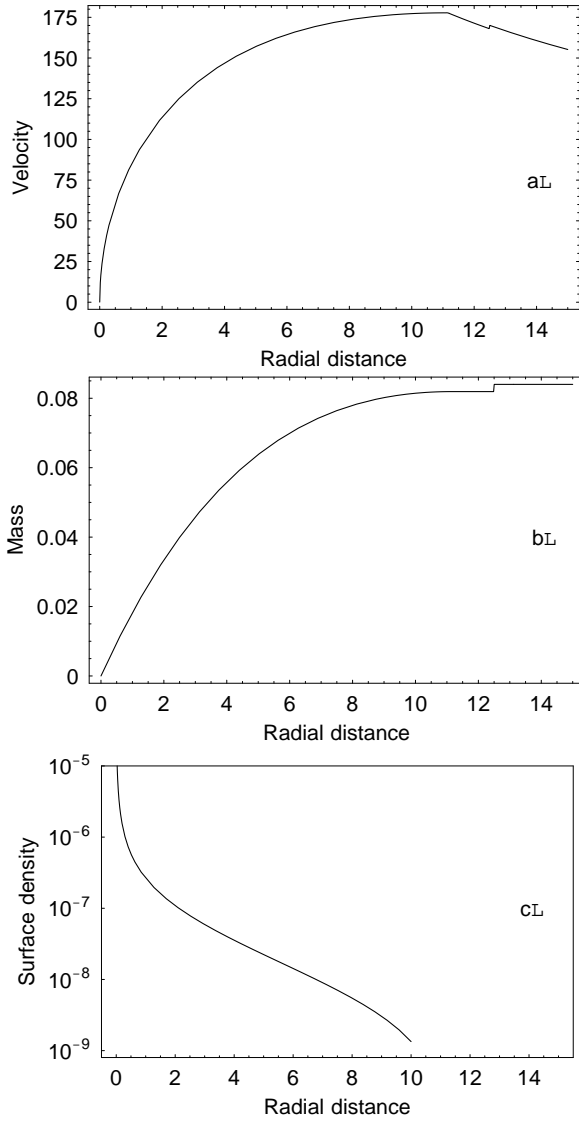


FIG. 2 Model of spiral galaxy with an external orbiting star; a) rotation velocity in Km/s, b) mass distribution in $10^{10}M_{\odot}$, c) surface density in M_{\odot}/pc^2 .

The integration constant

One is usually faced with the problem of determining the mass distribution for a galaxy whose rotation velocity has been measured and not with the reverse problem shown as example in the previous section. The integration poses the problem of determining the integration constant; it must also be performed by numerical methods, because a good analytical fit to a rotation curve is seldom possible.

The previous example showed that a rotation curve starting from the center with a finite slope will lead to a singularity; the same conclusion could be drawn from a careful analysis of Eq. (10). When performing a numerical integration it will not be possible to start integrating from $r = 0$, due to the expected singularity. A good choice for an integration constant is then the mass internal to the radius chosen for the start of

the integration procedure. The mass internal to a chosen radius resolves the singularity by stating that the integrated mass up to that radius is one adjustable parameter but the dynamics internal to that radius is unknown.

The next example is designed to show the influence of the integration constant in the final surface density curve and to explain the authors' criteria in deciding which particular value to choose for the constant in any given situation. An analytical rotation curve is assumed, which was chosen to fit very closely the measured curve for DDO 154, Fig. 6. The chosen curve is defined by the relation

$$v = 31.0r - 12.1r^{1.358}, \quad (30)$$

with v in km/s and r in kpc; for the rotation curve plot see the solid line in Fig. 6.

The rotation curve was integrated numerically from a radius of 10pc and the mass internal to this radius was given the values of $1.203 \times 10^7 M_{\odot}$ and $1.17 \times 10^7 M_{\odot}$; the resulting mass distributions are shown in Fig. 3 a) where the solid line is for the higher integration constant. The standard procedure was used for the determination of surface densities associated with both mass distributions and the results are plotted on graph b) in the same figure.

It is clear from the analysis of the plots, that the solid lines and the higher integration constant are to be chosen if we have reason to believe that the galaxy's edge is somewhere around 7.6kpc while the lower integration constant would set the edge at 6.3kpc. In spite of some uncertainty there may be about the edge distance, it can be seen that the total mass estimation and the slope of the surface density are relatively insensitive to the choice of internal mass within "reasonable" limits.

B. The central singularity

The theoretical difficulties associated with the nucleus and the appearance of a central singularity have been briefly mentioned on the discussion of the reversed example; this question will now be examined with greater detail.

The rotational velocity is related to the mass profile by Eq. (10). The bracket on this equation must remain positive at all times or the velocity will evaluate to an imaginary value. If we assume that the mass profile starts with a power law such as $M = m_0 r^{\nu}$, it is required that $\nu < 1$ in order to guarantee that velocity evaluates to a real value.

The surface density is given by the derivative of mass divided by $2\pi r$ and so it is $\sigma = \sigma_0 r^{\nu-2}$, meaning that the surface density will always have a negative exponent near the center and so the singularity can't be avoided. If the mass distribution starts exponentially the result is still the same, leading to the conclusion that a gravity driven system must have central singularity.

The singularity can be avoided by consideration of other types of interaction besides gravity. For instance, a rigid body nucleus would supply the necessary central mass for the integration process, without leading to singularity. Obviously

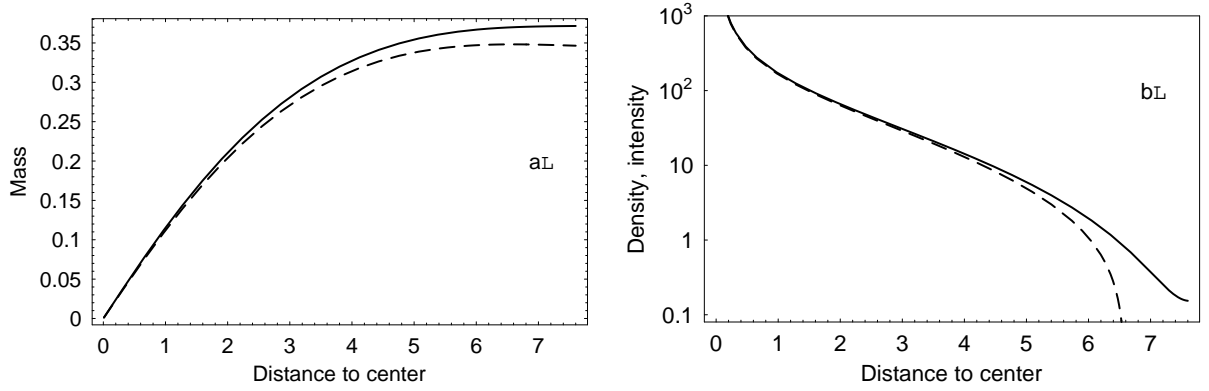


FIG. 3 Model of galaxy based on an analytical rotation curve (see text); the solid lines are consistent with the galaxy's edge being at 7.6 kpc, while the dashed lines set the edge at 6.3 kpc.

a rigid body can't be maintained by gravity alone but as distances decrease one inevitably has to consider electromagnetic and even strong forces, so there is nothing physically wrong with the fact that the present model must be applied only from a finite distance to the center.

In the present work, with one exception, all integrations were performed from 10 pc and the mass internal to this distance was used as integration constant; this will be given by the corresponding internal surface density.

C. Edge detection

Once the mass profile of a galaxy is known it is very easy to define its edge; one simply zeroes the derivative of the mass profile and considers this to be the edge. Physically this procedure is perfectly justified because mass must grow monotonically and stop growing gracefully at the edge. The problem, though, is usually the reverse because the mass distribution is the unknown, which one is trying to find based on rotation curves and information about surface density. The integration of a rotation curve introduces an integration constant, under the form of a mass internal to a chosen radius, which controls where the mass distribution is going to reach its maximum.

The decision about the integration constant can be replaced by a decision about where the edge is located and this must be reached from analysis of available surface densities data or directly from the rotation curve. The latter is not normally sufficient, as most rotation curves have a very flat end, making it extremely difficult to decide where mass really ceases to be present. It is important, then, to find some criterion for edge detection based on surface densities.

We will use Eq. (10) and rewrite the bracket in terms of surface density

$$M - r \frac{dM}{dr} = M - 2\pi\sigma r^2. \quad (31)$$

If the density is zero we are definitely outside the galaxy and the velocity follows the Keplerian rule. The problem resides then in the comparison between the two bracket terms, which

can alternatively be put as

$$\sigma \ll \frac{M_t}{2\pi r_0^2}. \quad (32)$$

In words it can be said that the edge is reached if the surface density becomes very small compared to the average surface density.

It would be nice to have a fixed edge threshold for the surface density and then apply this to all the measured mass densities to decide upon edge location. Based on the argument above this would suppose a universal average surface density, which we can't confidently assume; on the other hand, the fact that MOND can be applied with success to a large number of galaxies seems to indicate some constancy of the average surface density. The four galaxies covered in the present study have average surface densities spanning a range of $7\times$, the highest one being M31 with an average surface density of $65 M_\odot/\text{pc}^2$. Far away from the center, the only surface data available usually pertain to atomic hydrogen; these are then the data that must be used for edge location by comparison to the average surface density.

Eq. (32) can be given a physical interpretation by means of a few substitutions. The surface density can be replaced by the density ρ multiplied by the disk thickness $2T$. Since we are dealing with an atomic hydrogen gas, the density can be further replaced by the mass of the hydrogen atom divided by the cube of the average distance between atoms: $\rho = m_H/d_0^3$. Making those replacements the edge criterion becomes

$$\frac{m_H}{d_0^2} \times \frac{2T}{d_0} \ll \frac{M_t}{2\pi r_0^2}; \quad (33)$$

the fraction on the first member has been split in two for ease of interpretation.

In Eq. (33) $2T/d_0$ is the number of hydrogen atoms in a column of height $2T$ and square section d_0^2 , m_H/d_0^2 is proportional to the gravitational field due to one hydrogen atom and M_t/r_0^2 is proportional to the gravitational field of the galaxy. If both members were multiplied by $2Gm_H T/d_0$, the first member would represent the force of one column of atoms into a neighboring column, while the second member would

TABLE I Edge placement H_I density thresholds for the four galaxies studied in this work. Mass is in $10^{10} M_\odot$, radius in kpc and threshold in M_\odot/pc^2 .

Designation	Mass	Radius	Threshold
M31	27	26	0.64
NGC 3109	1.5	12	0.13
DDO 154	3.6	7	0.12
NGC 247	2.8	10	0.45

represent the force of the galaxy into the same column, apart from the 2π factor. The equation then states that the hydrogen atoms are not part of the galaxy, they gravitate as free particles, if the gravitational force of the galaxy prevails over the interatomic forces; on the contrary, when interatomic forces prevail over the galactic force the atoms behave like a gas and we have a continuum for the integration of the velocity curve.

The authors will use a uniform criterion based on an H_I 200 times lower than the average density of the galaxy for edge placement; table I lists all the thresholds used in the present study.

D. Tully–Fisher Relation

It has been known since 1977 that there is a relationship between the maximum rotational velocity of spiral galaxies and their luminosity; this relation, established by Tully and Fisher (Tully and Fisher, 1977), has the form

$$v_m^\eta \propto L, \quad (34)$$

where η can take values between 2 and 2.5. Tully and Fisher suggest that one should consider the higher value but they also say that different assumptions can lead to other values. A more recent survey of a large number of galaxies extends the exponent range of the observed blue Tully-Fisher exponent to a minimum of 1.51 and a maximum of 3.10 (Giuricin *et al.*, 1986). Tully-Fisher relation, as the equation above is known, is purely empirical and so far no one has been able to establish an underlying physical support for it. The authors believe that such support can be found within the framework of their proposed new law; such is the subject of the present section.

Most velocity curves exhibit a steep rise near the center, becoming gradually stationary at the last measured point. It is reasonable to assume that the last measured point is near the galaxy's edge, this being the distance where mass raises to its maximum value; this assumption is further supported by the examples given in the previous section. One can then associate the maximum rotation velocity to the edge velocity, this being identified by the mass distribution maximum; this condition can be inserted in Eq. (10) to find an expression for the edge velocity, similarly to the procedure used in Sec. IV. Zeroing the mass derivative in the referred equation

$$v_m^2 = \frac{M_t}{r_0}, \quad (35)$$

with r_0 the edge radius. Inserting Eq. (34)

$$L^{2/\eta} \propto \frac{M_t}{r_0}; \quad (36)$$

defining the average surface density as $S = M_t/2\pi r_0^2$

$$L^{2/\eta} \propto S r_0. \quad (37)$$

This is not an unnatural conclusion because it states that the total number of stars is proportional to the surface density, multiplied by the radius and raised to a power slightly larger than unity. Eq. (37) governs star production; if it is assumed that most of the galaxy's mass is in the form of a gas cloud, then it is to be expected that star production grows with the gas density and with the size of the galaxy. The actual value of the exponent can account for a number of things, namely the physical mechanisms of star production, the galaxy's shape, etc.

E. Normal Brightness Galaxies

A more stringent test results from modeling the mass distribution of an observed galaxy from the velocity data and matching it to the corresponding luminosity data. One such galaxy is Andromeda, known as M31, which was studied in 1969 by V. Rubin and W. Ford (Rubin and Ford, Jr., 1970). Photometric data for the same galaxy was published earlier by G. de Vaucouleurs (de Vaucouleurs, 1958) and used by Rubin and Ford in the cited study. Later this galaxy was the object of numerous studies but reference will be made here especially to (Sofue and Kato, 1981), which provides data on H_I density and rotation curves are also taken from (Braun, 1991) (molecular hydrogen) and from (Kent, 1989) (atomic hydrogen). From Rubin and Ford's study one concludes that M31's rotation velocity can conveniently be modeled by the thin lines in Fig. 4 a). The solid line curve is a good polynomial fit to the data, while the dashed curve was proposed by the study's authors to avoid the meaningless negative surface densities that resulted from the application of the better fitted one (Rubin and Ford, Jr., 1970). The same figure shows the H_{II} circular rotation curve from (Braun, 1991), where the two last points have been slightly adjusted up within the error bars. The adjustment was needed because the end slope of Braun's curve is too steep and would lead to an unreasonable surface density. Finally, the figure shows the composite H_I rotation curve from (Kent, 1989), extending from 4 to 30 kpc.

Total mass and mass distribution:

Modeling was performed separately for the H_I and the optical curves. In order to find the mass distribution the rotation curve from Kent and Braun were squared and inserted in the first member of Eq. (10), following which a numerical integration was performed. In the case of the Kent curve the integration was performed from the first point in the curve at 4 kpc and the mass internal to that distance was given

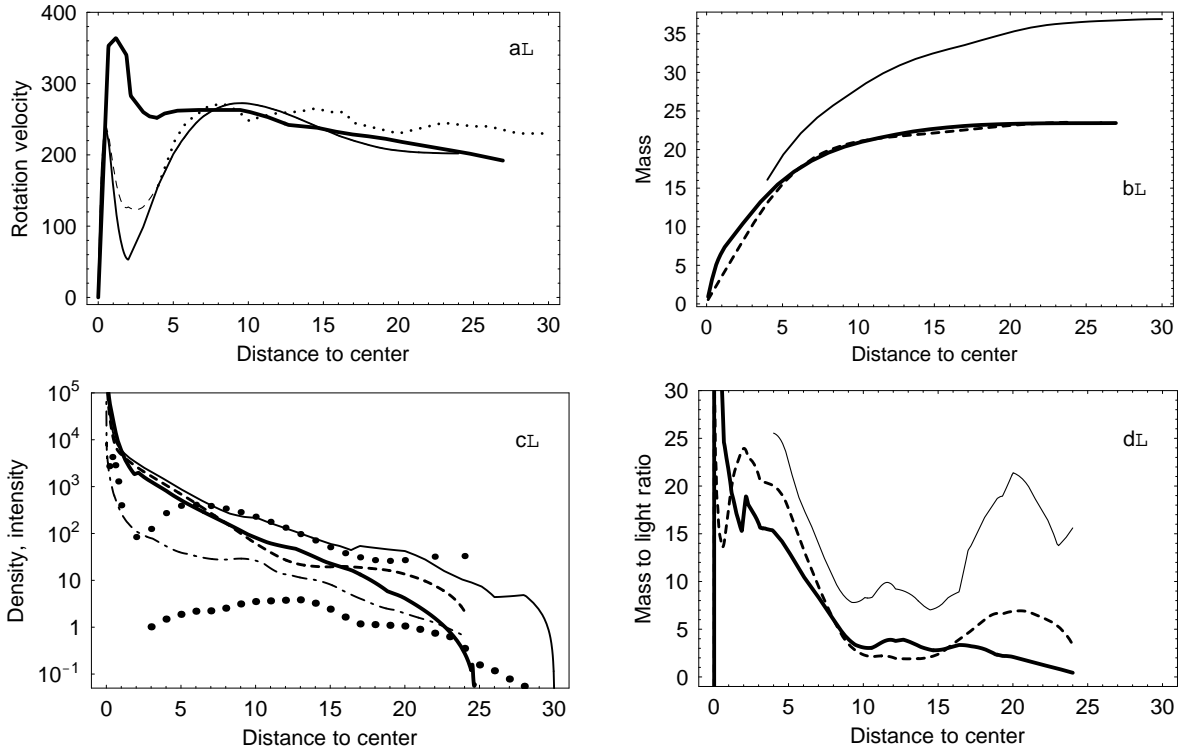


FIG. 4 Model of M31 galaxy; distance to center in kpc: a) rotation velocity in Km/s according to Braun (heavy line) (Braun, 1991), to Kent (dots) (Kent, 1989) and to Rubin and Ford (thin line) (Rubin and Ford, Jr., 1970); the dashed line avoids negative surface density; b) mass distribution in $10^{10} M_{\odot}$; thin line is for Kent's curve, heavy line is for Braun's curve and dashed line for Rubin and Ford's model 5; c) surface density derived from Kent's rotation curve (thin line), Braun's curve (heavy line), from Rubin and Ford's curve (dashed line), light intensity (dash dot), surface density from Rubin and Ford's paper (small dots) and H_I density (large dots); vertical scale in suns/pc^2 ; d) mass to light ratio from Kent's curve (thin line), Braun's curve (heavy line) and from Rubin and Ford's curve (dashed line); vertical scale in M_{\odot}/L_{\odot} .

a value of $1.6 \times 10^{11} M_{\odot}$, chosen such that the mass distribution had a stationary point at 30 kpc. If the rotation curve had been extrapolated to the center following Rubin and Ford's curve, the central surface density would have been set at $1.99 \times 10^6 M_{\odot}/\text{pc}^2$. The resulting mass distribution is plotted in Fig. 4 b) (thin line). Analysis of the corresponding surface density, Fig. 4 c), shows that the edge is located too far out but since the rotation curve does not exhibit a Keplerian tail it was impossible to follow the authors' criterion for edge placement. A similar procedure was then followed for Braun's rotation curve, with the central surface densities set to $2.96 \times 10^6 M_{\odot}/\text{pc}^2$, so that the edge would be very near 25 kpc, where the H_I density is approximately $0.64 M_{\odot}/\text{pc}^2$ and the curve starts its Keplerian behaviour. Rubin and Ford's curve was integrated with a central density of $1.78 \times 10^6 M_{\odot}/\text{pc}^2$, assuming that it could be extended to an edge near 25 kpc. The total mass estimated from H_I curve is approximately $3.7 \times 10^{11} M_{\odot}$, while the optical curves underestimate this value, setting the total mass at approximately $2.3 \times 10^{11} M_{\odot}$. Rubin and Ford found a mass at 24 kpc of about $1.8 \times 10^{11} M_{\odot}$ but rising linearly with distance; they also pointed out that if one uses Brandt rotation formula the mass at this distance will be $2.1 \times 10^{11} M_{\odot}$ and the total mass of the galaxy $3.7 \times 10^{11} M_{\odot}$. It follows that the authors' model predicts a total mass that is in excellent agreement with the

masses predicted by other models but yields a much more natural mass distribution; dark matter is here located centrally and not in a halo.

Surface density vs. luminosity profile:

Naturally, as M31 has a more or less elliptical shape, Eq. (29) can only give an approximation of real surface density but it is still useful both for decision about the integration constant and for comparison to the luminosity profile and H_I density. The mass distributions from Fig. 4 b) were thus derived and divided by $2\pi r$, with the result being used as a representations of the galaxy's surface density. Fig. 4 c) shows the calculated surface density for the three mass distributions; it makes very clear that the option taken for the central surface density actually leads to a zero surface density at 30 kpc, the authors' adopted edge.

In order to plot a luminosity versus distance curve, the tables from de Vaucouleurs (de Vaucouleurs, 1958) were used; the luminosity values along the minor and major axes were averaged at the same distance and the average was used as the galaxy's luminosity. The integrated luminosity of the galaxy can be found in de Vaucouleurs to be $1.4 \times 10^{10} L_{\odot}$. In order to give meaningful units to the luminosity profile this was multi-

plied by $2\pi r$, integrated and the result was made to match the integrated luminosity.

The luminosity profile as well as H_I density are also plotted in Fig. 4 c). The surface densities and luminosity are essentially following each other except for reasonable variations in the proportion of luminous matter and for the sharp increase in surface density, already discussed, near the center of the galaxy. H_I density is always comparatively low and below the calculated surface density. Mass to luminosity ratio is plotted in Fig. 4 d) in linear scales for all the mass distributions.

It will be noted that Rubin and Ford's paper surface density based on Newton's Law (Table 3, Model 6 as reproduced here in Fig. 4 c)) has bulges near the center and around 6 kpc, while tapering off to a low but constant value. None of these features appears to have any physical meaning when compared to the almost straight exponentially decreasing luminosity profile. These are most likely artifacts resulting from the velocity bulges of Fig. 4, which Newton's Law fails to smooth out. The authors are advancing that such artifacts are at the origin of the Dark Matter hypothesis.

F. Low Surface Brightness Galaxies

The authors chose for this study three galaxies whose data could easily be found on the internet and showed characteristics that would effectively test their model.

NGC 3109 spiral

This galaxy was studied by Jobin and Carignan (Carignan, 1985a; Jobin and Carignan, 1990) where data can be found for rotation velocity, luminosity and H_I density, allowing for a complete test of the authors' model.

Fig. 5 a) shows the interpolated rotation curve; at 8 kpc the velocity is apparently still rising slowly, giving an indication that the galaxy's edge is further beyond; the same indication is inferred from the fact that H_I data is available up to 12 kpc, as shown in Fig. 5 c). For consistency with their edge placement criterion, the authors extrapolated the rotation curve to 12.5 kpc.

A procedure in all respects similar to the one described for M31 was used to find the mass distribution, which is shown in Fig. 5 b); the choice of $8.1 \times 10^4 M_\odot/\text{pc}^2$ for the central density allows the surface density to match H_I density in Fig. 5 c) at the last measured point. The total mass can be estimated as approximately $1.45 \times 10^{10} M_\odot$, a value which is to be compared with $0.9 \times 10^{10} M_\odot$ resulting from Carignan's model at 8.3 kpc (Carignan, 1985a). Carignan's mass is naturally growing linearly with distance at 8 kpc.

In Fig. 5 c) the surface density is shown together with the light intensity and H_I density. The absolute values for light intensity were obtained from the luminosity data, combined with the indication from Ref. (Carignan, 1985a) that the corrected central brightness is $23.17 \text{ mag/arcsec}^2$ and corresponds to an intensity of $34.1 L_\odot/\text{pc}^2$. As with M31 it is seen

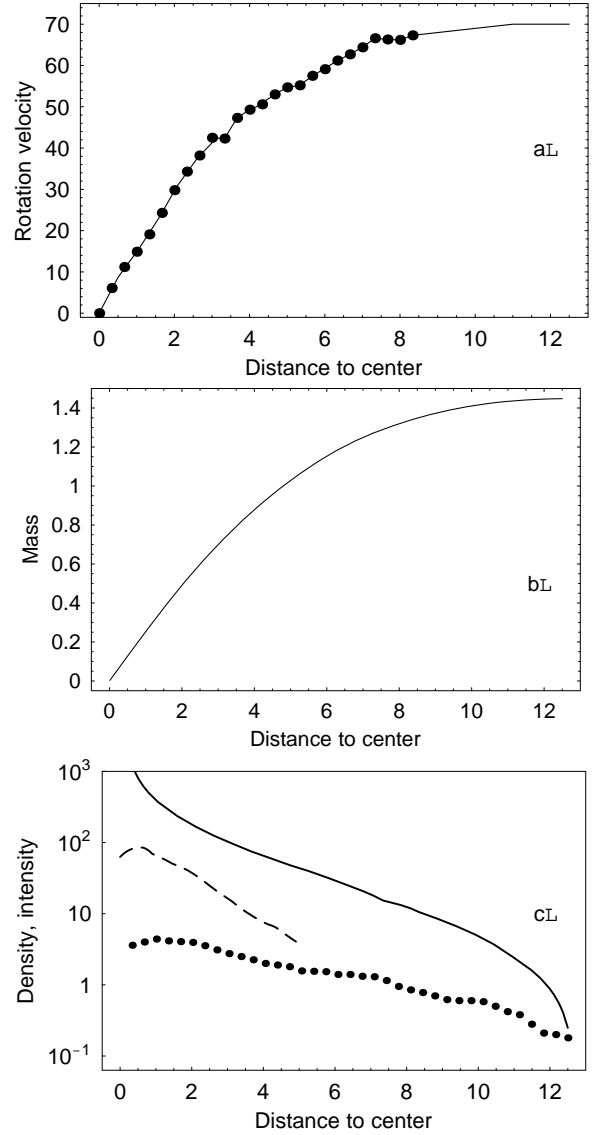


FIG. 5 Model of the NGC 3109 galaxy with distance in kpc: a) rotation velocity in Km/s. b) mass distribution in $10^{10} M_\odot$. c) surface density (solid line), light intensity (dashed line) and H_I density (dots) in suns/pc^2

that the mass to light ratio is approximately constant, with values between 4 and 8 in the range 0.7 to 4.8 kpc. If H_I density is taken into consideration the slight M/L variation can be explained as well as the extension of the surface density beyond the light detection limit. It appears that NGC 3109 can be modeled as a single disk with dark matter distributed proportionally to light and hydrogen rather than in halo. The M/L ratio is one subject of discussion later in this work.

DDO 154

DDO 154 is an interesting nearby dwarf namely because it may be one of the first systems where the edge of the mass

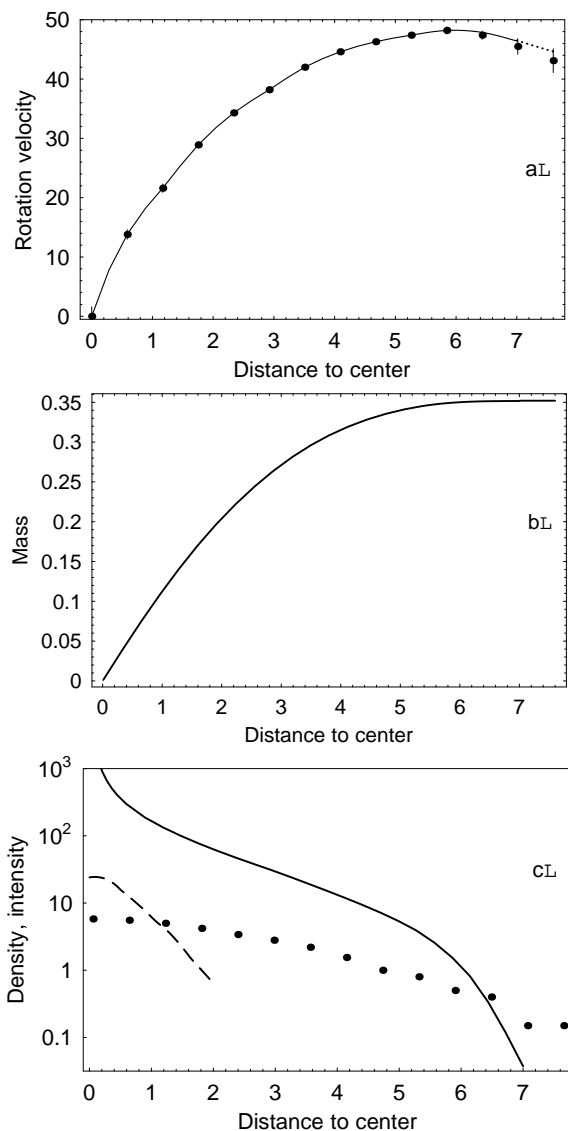


FIG. 6 Model of the DDO 154 galaxy with distance in kpc: a) rotation velocity in Km/s (see text for the explanation of the various symbols). b) mass distribution in $10^{10} M_{\odot}$. c) surface density (solid line), light intensity (dashed line) and H_I density (dots) in M_{\odot}/pc^2 .

distribution has been reached, which results from the fact that the rotation curve is declining for the highest radii (Carignan and Beaulieu, 1989). Fig. 6 a) shows the points from the rotation curve adopted in Ref. (Carignan and Beaulieu, 1989) with error bars. Fitting a smooth curve to the last points results in a negative slope to steep for an integration of the rotation curve to be performed after 6.3 kpc. In compliance with their edge placement criterion the authors chose an H_I density of $0.12 M_{\odot}^2/pc$ and a distance of 7 kpc for edge location, so that the rotation curve should be Keplerian after this distance. The non-Keplerian part of the fitted curve is shown by the solid line while the dotted line shows the Keplerian part. A slight adjustment was made within the error bars.

The integration procedure was similar to the previous cases and the resulting mass distribution and surface density are

shown in Fig. 6; the internal surface density was set to $3.78 \times 10^4 M_{\odot}/pc^2$. The total mass was estimated as $3.5 \times 10^9 M_{\odot}$, in excellent agreement with Carignan and Beaulieu's $3.9 \times 10^9 M_{\odot}$ (Carignan and Beaulieu, 1989). The Keplerian fit model can be seen as a situation similar to what was described in the reversed example model in page 4, with the farthest hydrogen atoms being beyond the galaxy's edge and thus causing the sudden change in slope of the rotation curve. The outer curve is really stepwise Keplerian, as in the referred example, but the extremely small mass increases due to individual atoms make this consideration meaningless.

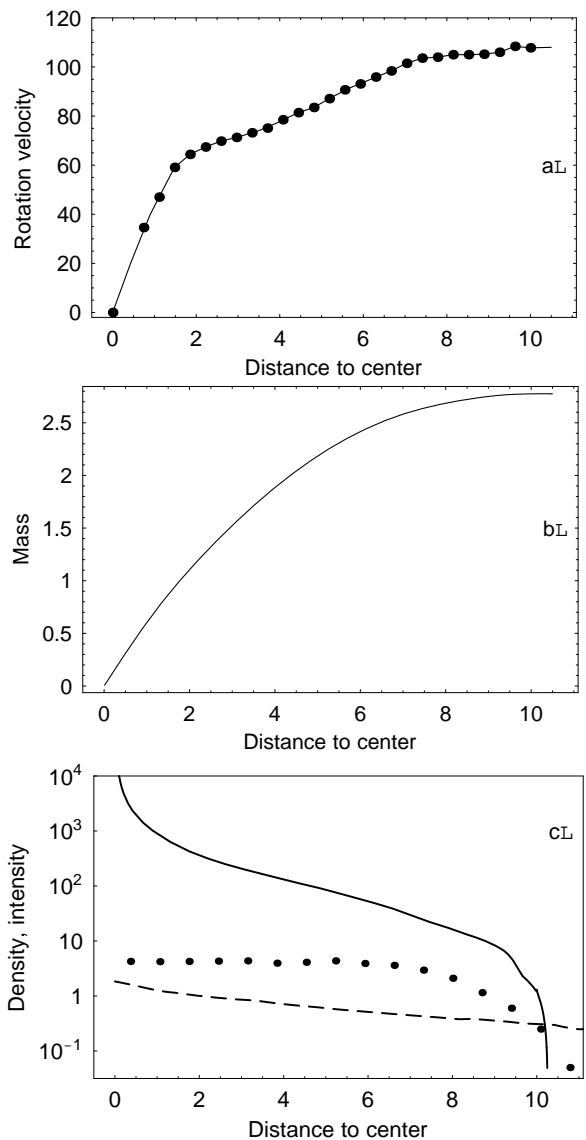


FIG. 7 Model of the NGC 247 galaxy with distance in kpc: a) rotation velocity in Km/s. b) mass distribution in $10^{10} M_{\odot}$. c) surface density (solid line), light intensity (dashed line) and H_I density (dots) in M_{\odot}/pc^2 .

NGC 247

This galaxy is a member of the Sculptor group, located at an estimated distance of 2.53 Mpc (Carignan, 1985b; Carignan and Puche, 1990) and was chosen for the present study due to its low surface brightness, with $B(0)_c = 23.44 \text{ mag/arcsec}^2$, combined with very good resolution, allowing for an analysis without consideration of beam smearing effects, as could not be done for most low surface brightness galaxies.

One of the main features of this NGC 247 is the short extent of the H_I disk, resulting in brightness measurements that go well beyond the rotation curve. The authors chose to place the galaxy's edge at $n H_I$ density of 0.45 kpc, occurring at 10.2 kpc, and consistently extrapolated the rotation curve assuming that the extended luminosity profile was attributable to external stars, such as the one in the reversed example.

Fig. 7 c) shows the calculated surface density compared with the light intensity and H_I density, bringing to evidence that there is a discrepancy between the slopes of the three curves, which calls for some dark matter concentrated near the nucleus; M/L can't be maintained to the end of the brightness curve. Carignan (Carignan, 1985b) mentions that internal absorption could be quite important for this galaxy, due to its large inclination; this fact could well help explain the high slope of the surface density curve. The central surface density was set at $2.00 \times 10^5 M_\odot/\text{pc}^2$ for integration and the total mass is estimated by the authors as $2.8 \times 10^{10} M_\odot$. Carignan and Puche estimate a mass of $2.6 \times 10^{10} M_\odot$ within 7.35 kpc; this excellent agreement is remarkable in view of the totally different models used in the two studies. The extended brightness curve is believed to be due to external stars; information is needed about the rotation velocity of these stars, which is expected to follow a Keplerian rule.

VI. DISCUSSION

The authors propose a model for galaxy dynamics which successfully explains several observed features of different types of galaxies; this model is based on a postulated space metric for general relativity but it is still a space-time curvature model and thus gravity driven. The model assumes that the galaxy behaves like a continuum where the gravitational attraction on one particle is transmitted to all others; this is shown to hold while the interatomic interactions are strong but ceases to be true once the atoms are so far apart that the galaxy's gravity dominates over the forces between atoms. Beyond this point atoms become essentially isolated particles and follow the Keplerian rule. The criterion for transition between collective behaviour and isolated particles was defined in terms of atom separation and disk thickness, the latter being rather difficult to assess very near the edge, so a trial and error procedure could not be avoided.

The model breaks down at the center, as a gravitational model is expected to do. It is quite understandable that any body's orbit must have a radius that is large compared to the body's dimensions; this is true at all levels and as one proceeds inwards in the galaxy, the orbiting bodies and particles

must have smaller and smaller dimensions. One sees successively the impossibility of stars, dust particles, atoms and even elementary particles. Naturally there are several possibilities, involving electromagnetic and strong interactions, which must be used where the gravitational model no longer holds.

The authors would like to make a daring suggestion of a totally different method to address the problem discussed above, which appeals to the 4-dimensional optics theory (Almeida, 2002a,b). Within this theory the galaxy will be seen as a waveguide in 4-dimensional space, described by a single function, removing the distinction between gravity and the other interactions and avoiding the central breakdown. The galaxy's edge is then understood as the point where the guided field ends and evanescent field begins. The metric that was postulated in the present paper is actually a consequence of the theory and all mass (inertial or gravitational) is undistinguishable from space curvature.

VII. CONCLUSION

Galactic mass distributions inferred from observed luminosities can match observed peripheral velocities without appeal to dark matter provided a space metric different from the Schwarzschild solution of Einstein's equation is considered. This metric leads to Newton and MOND's gravity laws without having to adjust parameters of the theory. The velocity profile and integration constant choices tie the problem to a specific galaxy with its specific form and mass, which are not parameters of the theory as the Dark Matter and MOND approaches need, no more than mass adjustment and distances in Newton's Law. The metric is not only justified by observations but may be an additional tool for the evaluation of the dynamics of galaxies. A future study will also investigate its theoretical meaning for the age-old puzzling connection of the vacuum (space) with its content, be it masses or fields.

References

- Abramowitz, M., and I. A. Stegun, 1970, *Handbook of Mathematical Functions* (Dover pub., N. York), 9th edition.
- Almeida, J. B., 2001, A theory of mass and gravity in 4-dimensional optics, eprint physics/0109027.
- Almeida, J. B., 2002a, K-calculus in 4-dimensional optics, eprint physics/0201002.
- Almeida, J. B., 2002b, Prospects for unification under 4-dimensional optics, eprint hep-th/0201264.
- Braun, R., 1991, *Astron. J.* **372**, 54.
- Carignan, C., 1985a, *Astrophys. J.* **299**, 59.
- Carignan, C., 1985b, *Astrophys. J. Suppl. Ser.* **58**, 107.
- Carignan, C., and S. Beaulieu, 1989, *Astrophys. J.* **347**, 760.
- Carignan, C., and D. Puche, 1990, *Astron. J.* **100**(3), 641.
- de Vaucouleurs, G., 1958, *Astrophys. J.* **128**, 465.
- Giuricin, G., F. Mardirossian, and M. Mezzetti, 1986, *Astron. Astrophys.* **157**, 400.
- Jobin, M., and C. Carignan, 1990, *Astron. J.* **100**(3), 648.
- Kent, S. M., 1989, *Publ. Astron. Soc. Pac.* **101**, 489.
- Martin, J. L., 1988, *General Relativity: A Guide to its Consequences for Gravity and Cosmology* (Ellis Horwood Ltd., U. K.).

- Milgrom, M., 1983a, *Astrophys. J.* **270**, 371.
- Milgrom, M., 1983b, *Astrophys. J.* **270**, 365.
- Rubin, V. C., and W. K. Ford, Jr., 1970, *Astrophys. J.* **159**, 379.
- Rubin, V. C., W. K. Ford, Jr., and N. Thonnard, 1978, *Astrophys. J.* **225**, L107.
- Sanders, R. H., 1996, *Astrophys. J.* **473**, 117.
- Schwarzschild, K., 1916, in *Sitzungsberichte der Königlich Preussischen Akademie der Wissenschaften Zu Berlin, Phys.-Math. Klasse*, pp. 189–196, english translation, eprint physics/9905030.
- Silk, J., 1997, *A Short History of the Universe* (Scientific American Library, N. York).
- Sofue, Y., and T. Kato, 1981, *Publ. Astron. Soc. Jpn.* **33**, 449.
- Tully, R. B., and J. R. Fisher, 1977, *Astron. Astrophys.* **54**, 661.